

Wavepackets falling under a mirror

G. Kälbermann*

Soil and Water dept., Faculty of Agriculture, Rehovot 76100, Israel

October 31, 2018

Abstract

We depict and analyze a new effect for wavepackets falling freely under a barrier or well. The effect appears for wavepackets whose initial spread is smaller than the combination $\sqrt{\frac{l_g^3}{|z_0|}}$, between the gravitational length scale $l_g = \frac{1}{(2 m^2 g)^{1/3}}$ and the initial location of the packet z_0 . It consists of a diffractive structure that is generated by the falling and spreading wavepacket and the waves reflected from the obstacle.

The effect is enhanced when the Gross-Pitaevskii interaction for positive scattering length is included.

The theoretical analysis reproduces the essential features of the effect. Experiments emanating from the findings are proposed.

PACS 03.65.Nk, 42.25.Fx, 0.75.F

*e-mail address: hope@vms.huji.ac.il

1 Introduction

In the past years we have described a new phenomenon called : *Wavepacket diffraction in space and time*. [1]-[5]. The phenomenon occurs in wavepacket potential scattering for the nonrelativistic Schrödinger equation and for the relativistic Dirac equation. The effect consists in the production of a multiple peak structure that travels in space and persists. This pattern was interpreted in terms of the interference between the incoming spreading wavepacket and the scattered wave. The patterns are produced by a time independent potential in the backward direction, in one dimension, and, at large angles, in three dimensions. The multiple-peak wave train exists for all packets, but, it does not decay only for packets that are initially thinner than $\sqrt{\frac{w}{q}}$, where w is a typical potential range or well width and q is the incoming average packet momentum. For packets that do not obey this condition the peak structure eventually merges into a single peak. The effect appears also in forward and backward scattering of wave packets from slits. [5]

The experimental breakthrough of Bose-Einstein condensation in clusters of alkali atoms [6, 7] ¹ lead to the reinvestigation of the influence of the earth's gravitational field on the development of a quantum system.

Gravity is currently being advocated as a mean to allow the extraction of atoms from the condensate for the realization of an atom laser continuous output coupler . [8, 9, 10] Despite the weakness of the gravitational force on earth, it has a major influence on atoms that are cooled to microKelvin temperatures. It is then necessary to include the effects of gravity in theoretical calculations with condensates.

Many other gravitational effects with quantum systems are being considered nowadays, such as bound states of neutrons in a gravitational field above a mirror, [11], or the use of the coherence properties of condensates to serve as interferometers in the presence of gravity [12, 13].

The Bose-Einstein condensate in a magnetic trap is in reality a wave packet. To the extent that decoherence effects are not dominant, it is expected to evolve in a gravitational field in the same manner as a Schrödinger wave packet. In the present work we investigate the effects of gravity on falling packets.

It will be shown numerically and analytically that packets falling *under* an obstacle but, free from below, display distinctive quantum features due to their wave nature.

The Schrödinger wavepackets not only fall, in accordance with the equivalence principle, but also spread. The thinner the initial extent of the packet the broader the spectrum of momenta it carries. Consequently, it will generate many more components able to reflect from the obstacle, be it a well or a barrier. These reflected waves will interact with the spreading and falling packet.

There is crossover length scale, at which the interfering pieces start to produce a diffrac-

¹A comprehensive bibliography on Bose-Einstein condensation may be found at the JILA site <http://bec01.phy.GaSoU.edu/bec.html/bibliography.html>

tive coherent structure that travels in time, analogous to the effect of wave packet diffraction in space and time previously investigated.[1]-[5]

This length scale is the gravitational scale $l_g = \frac{1}{(2 m^2 g)^{1/3}}$. For Sodium atoms it is about 0.73 microns, while for Hydrogen it is 5.86 microns.² For packets *initially* narrower than a proportion of this scale, the effect is extremely evident, and gets blurred the wider the initial packet. This effect may be observed with the same setup as the one used in Bose-Einstein condensation experiments, provided pencil-like, thin packets are produced and allowed to fall under a roof.[12]

We will provide analytical approximations to the exact solution of the problem that reproduce quite satisfactorily the numerical results. In section 2 we present numerical results. Section 3 will deal with theoretical aspects. Section 4 summarizes the paper and provides concluding remarks regarding possible experiments.

2 *Packets falling under a roof*

Matter wave diffraction phenomena in time [14] induced by the sudden opening of a slit, or in space by fixed slits or gratings, are understood simply by resorting to plane wave monochromatic waves.

Atomic wave diffraction experiments [16], have confirmed the predictions of diffraction in time[14] calculations. These patterns fade out as time progresses.

The phenomenon of diffraction of wavepackets in space and time was presented in [1]-[5]. It consists of a multiple peak traveling structure generated by the scattering of initially thin packets from a time independent potential, a well, a barrier, or a grating. The condition for the pattern to persist was found to be

$$\sigma \ll \sqrt{\frac{w}{q_0}} \quad (1)$$

where σ is the initial spread of the packet, w is the width of the well or barrier and q_0 is the impinging packet average momentum. For packets broader than this scale the diffraction pattern mingles into a single broad peak.

The original motivation for the present work, was the addition of gravity to the potential affecting the packet propagation. As described above, the effects of gravity become increasingly relevant to the dynamics of packets in traps and elsewhere.

The educational literature abounds in works dealing with the dynamics of packets falling on a mirror. The so-called *quantum bouncer* [17] is a clean example of the use of the Airy packet in the treatment of the problem. The use of the Airy packet is straightforward above the mirror with the boundary condition of a vanishing wave function at the location of

² We use $\hbar = 1$, $c = 1$, and units of length in microns, of time in milliseconds, $g = 9.8 \frac{\mu}{(msec)^2}$.

the mirror, and, becomes a nice laboratory for the investigation of the quantum classical correspondence, revivals, the Talbot effect, etc. Falling packets were not studied, perhaps in light of the preconception that nothing interesting will be found besides the expected spread and free fall of the packet.

However, there is a surprise awaiting us here. This is not totally unexpected due to the wave nature of the packet that consists of modes propagating in both the downwards and the upwards direction. Analogous effects are apparent also when a packet propagates in parallel to a mirror without ever getting close to it.[18] Again the spreading and interference between the incoming and reflected waves produce a wealth of phenomena.

In this section, we present the numerical results for the falling of packets under a barrier or well using Gaussian wave packets. The use of Gaussian packets permits a straightforward connection to theoretical predictions.

The scattering event starts at $t = 0$ with a minimal uncertainty wavepacket

$$\begin{aligned}\Psi_0 &= A e^{i\alpha} \\ \alpha &= q(z - z_0) - \frac{(z - z_0)^2}{4\sigma^2}\end{aligned}\tag{2}$$

centered at a location z_0 large enough for the packet to be almost entirely outside the range of the potential. σ denotes the width parameter of the packet. $q = mv$ is the average momentum of the packet. The potential affecting the packet is a square well, the gravitational interaction, and eventually the Gross-Pitaevskii (GP) interaction, that subsums the effects of forces between the atoms in the condensate in the mean field approximation[19].

$$V = m g z + U \Theta(w/2 - |z - w/2|) + g |\Psi|^2\tag{3}$$

where m is the mass of the atom taken here to be Sodium, w is the width of the well or barrier, of depth or height U , and g is the strength of the GP interaction[19], which using the scattering length of Sodium and a typical number of atoms in a trap of the order of 250 atoms/ μ^3 yields $g \approx 25$ for a wavefunction normalized to one.

Figure 1 depicts the setup of the problem. A thin wave packet is initially located around a point $z_0 = -7\mu$ under a thick barrier, the mirror. The mirror could be any flat surface. We have represented the strength of the barrier by means of a square located above $z = 0$. The simplification of the present investigation assumes the mirror to be a finite width plate of thickness $t = 10\mu$ in the figure extending to a much larger distance along the x, y plane. For the one dimensional calculation we took a thin packet along the z axis of width $4\sigma \approx 0.4\mu$. It is supposed to be a pencil-like packet whose extension along the x, y plane is larger than the width, such that the quantum dispersion affects primordially the behavior of the packet along the vertical direction. In this direction, the packet falls freely. The interference between the packet components reflected from the barrier, upwards moving waves, and those that fall freely without reflection, the downward moving ones, will induce a diffraction pattern.

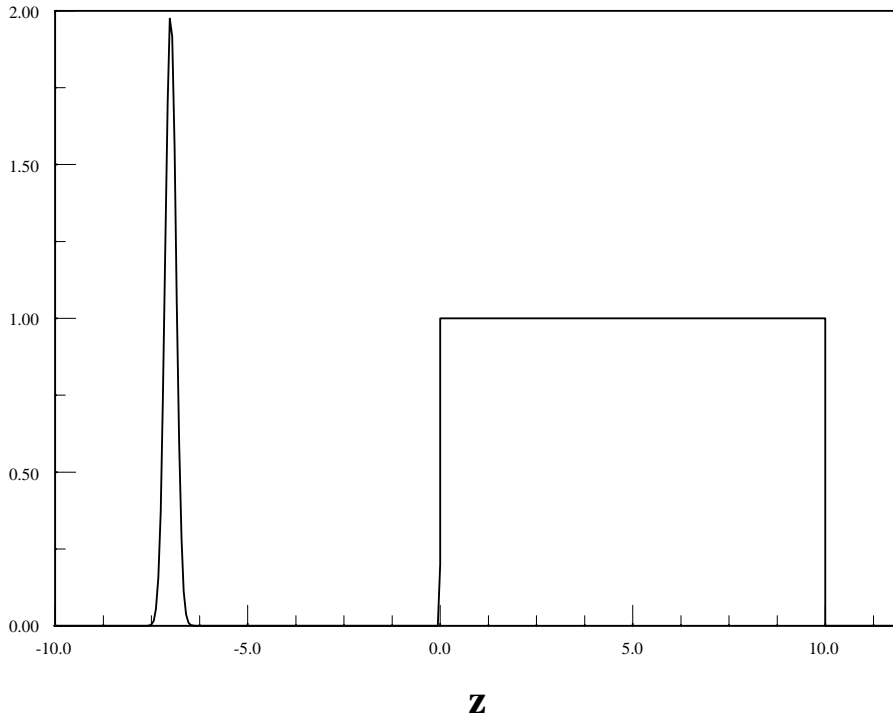


Figure 1: *Setup of the problem. The packet's initial location is $z_0 = -7\mu$. The mirror is depicted as a square of arbitrary height representing the strength of the repulsive potential. The mirror is located above $z = 0$ and its width is 10μ*

We will find that the contrast of the pattern depends crucially on the initial location of the packet and its width.

An ideal implementation of this setup would be to use a Bose-Einstein condensate optically trapped in a region below a plate. Suddenly stop the confining potential and let it fall freely under the plate.

The condition for the observation of the effect would be to produce a thin enough condensate. For repulsive Gross-Pitaevskii interactions as in Sodium, Rubidium, or Hydrogen, the width limitation is less stringent, as will be shown below. The extra repulsion of the interaction, on top of the quantum dispersion, effectively pushes the waves inside the condensate against the wall. It acts as if the packet was initially thinner than it actually is. In particular, for Hydrogen the initial width of the packet may be as large a few microns. In section 4 we make some further comments concerning the relevance of the effect for atom lasers.

The algorithm for the numerical integration of the Schrödinger equation of the present work is described in previous works.[1, 2, 3]. Flux conservation for initially normalized

packets and energy conservation require that

$$\begin{aligned}
1 &= \int_{-\infty}^{\infty} |\Psi(z, t)|^2 dz \\
E &= \int_{-\infty}^{\infty} \left[\frac{1}{2m} \frac{\partial \Psi(z, t)}{\partial z} \frac{\partial \Psi^*(z, t)}{\partial z} + (mgz + V(z) + \frac{g}{2} |\Psi(z, t)|^2) |\Psi(z, t)|^2 \right] dz \quad (4)
\end{aligned}$$

with E a constant independent of time.

The numerical runs presented below achieved an accuracy in the flux conservation of around 0.2%, while the accuracy in the energy conservation was around 2%. The wave function was also found to obey the Schrödinger equation to an accuracy better than the 1% level even at points near the edges of the integration range.

The only length scale appearing in the problem is easily derived from the Schrödinger equation to be l_g . For Sodium this is $l_g = 0.73\mu$

We consider the free fall of packets with initial widths σ smaller and larger than a fraction of l_g with or without the GP interaction. We take the barrier to have the fixed strength of $U = 10^6 \text{sec}^{-1}$ obtained from $U \approx \frac{4\pi a}{m} N$, with a , the scattering length of the Sodium-solid scattering and N the density of a typical solid. For the well we use a value taken from a van der Waals type of strength [20] at a distance of 1 nm, namely $U \approx -10^2 \text{sec}^{-1}$. We used a very high value for the attractive well strength, beyond the limit of applicability of the Lennard-Jones formula[20], to see whether even a large and unrealistic value for the attractive potentials influences the results as compared to the repulsive case.

Figure 2 shows the time evolution of a thin packet falling under a mirror. This is essentially what is expected to be observed in an actual imaging of a Bose-Einstein condensate falling freely under a mirror as a function of time. The figure shows the results for Sodium, however, as mentioned above the same will occur with a Hydrogen condensate, with much wider packets initially.

Figure 3 shows wide and thin packets profiles after 4 msec fall under a repulsive barrier.

The behavior of a thin packet is qualitatively different. A wide packet falls undistorted except for the natural spreading. A thin packet whose width is smaller than $\sqrt{\frac{l_g^3}{z_0}}$ (see below for the appearance of z_0 in the expression), possesses a distinctive diffractive structure. The rightmost (upper) edge of the structure resembles the Airy packet absolute value, however, the packet drops exponentially at large $|z|$ values, whereas the Airy packet diminishes as $|z|^{-1/4}$. In the next section we will address a theoretical approach to the problem. Approximate analytical solutions will be provided that reproduce the basic features of both the thin and wide packets.

In figure 4 we present an analogous picture for the case including the GP interaction. As expected[19], the distinctive feature of the inclusion of this interaction is an extra repulsive force, due to the positive scattering length, that enhances the broadening of the packet, and consequently the diffraction effect. As seen from the figure, for the same values of

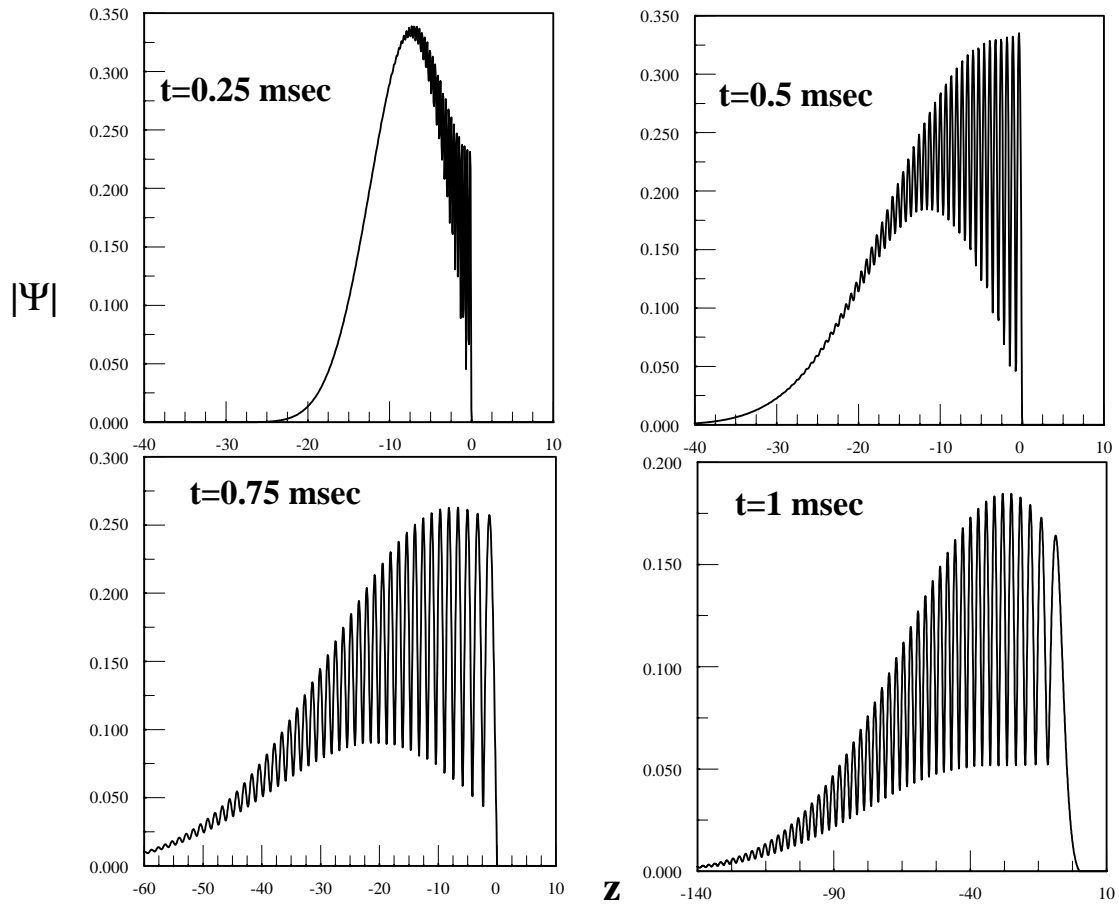


Figure 2: Time evolution of a packet profiles of initial location $z_0 = -7 \mu$ falling under the repulsive barrier (not depicted).

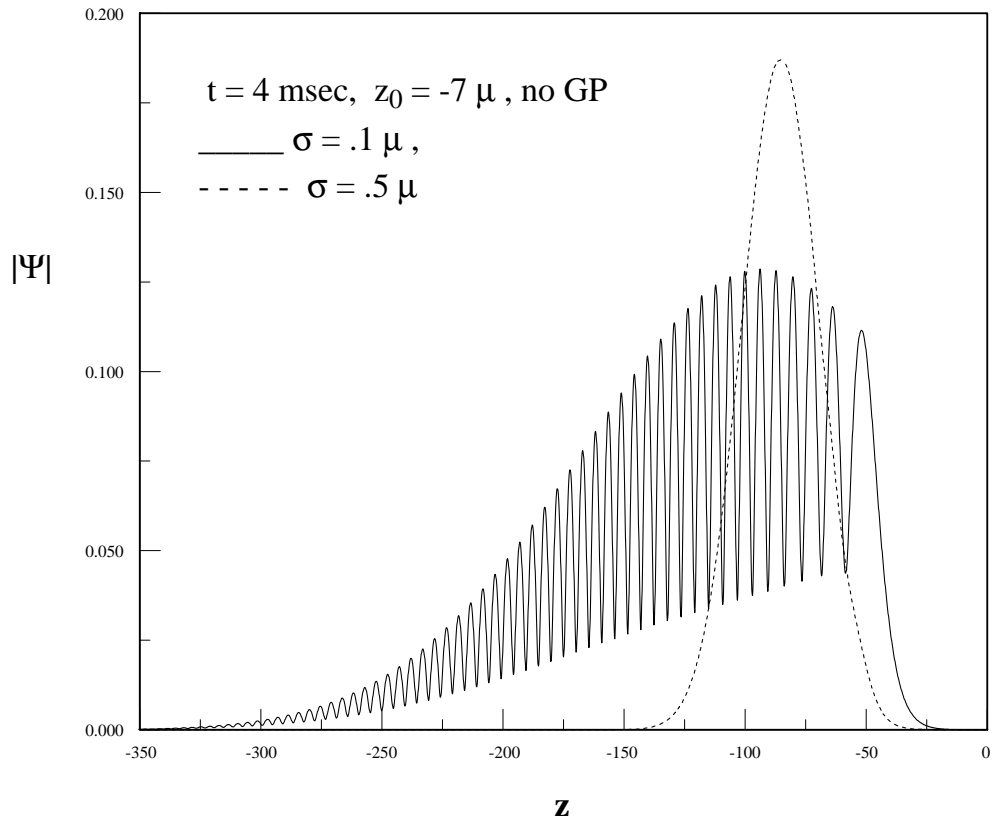


Figure 3: *Packets profiles of initial location $z_0 = -7 \mu$ after $t = 4 \text{ msec}$ falling under a repulsive barrier.*

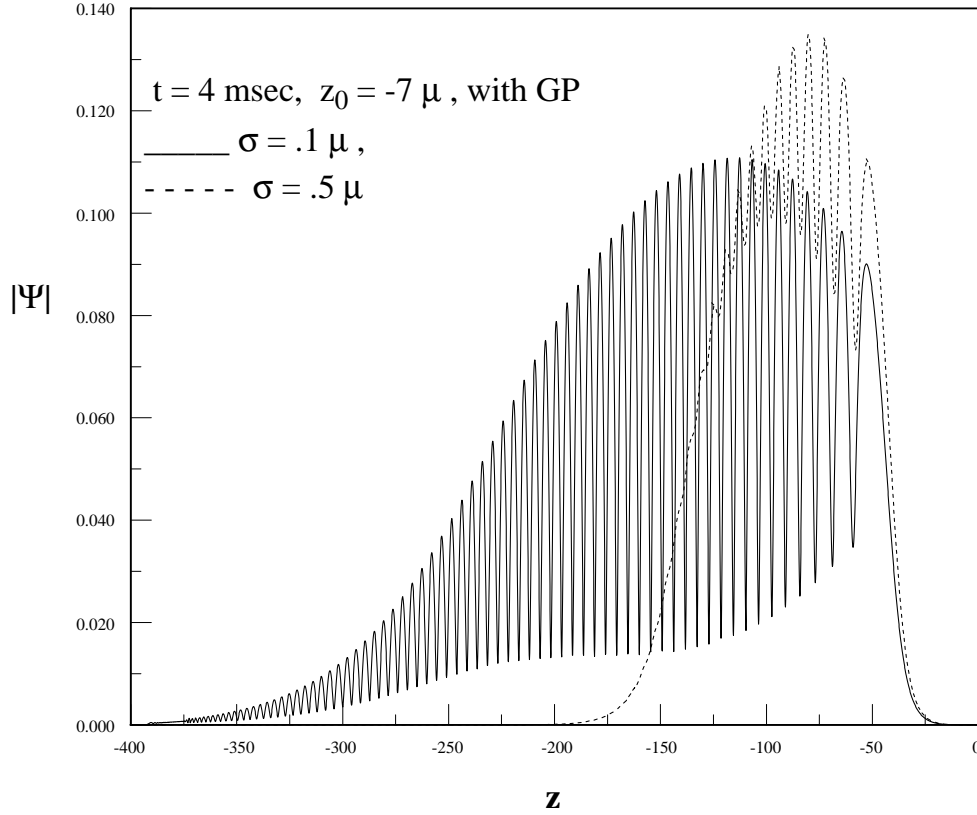


Figure 4: *Packets profiles of initial location $z_0 = -7 \mu$ after $t = 4$ msec falling under a repulsive barrier and subjected to the Gross-Pitaevskii interaction*

initial packet widths, the nonlinear repulsive interaction produces a much cleaner interference pattern than the case lacking it in figure 3.

Figure 5 depicts the influence of the GP interaction on the packets profiles for initially thin packets.

The GP force produces a diffractive structure that has a much starker contrast. Large momenta are excited by the repulsive interaction, producing a more effective superposition between incoming and reflected waves.

We argued that the appearance of a diffractive structure is determined by the ratio $\epsilon = \frac{\sigma}{\sqrt{\frac{l_g^3}{z_0}}}$. Figure 6 shows the results when this ratio is around 1. While the pattern has almost disappeared from the falling packet devoid of GP interaction, it has lost contrast, but not disappeared completely from the packet subjected to the GP force. ϵ is then the relevant ratio for the appearance of the diffractive structure.

Replacing the barrier by a well has no effect whatsoever for packets without initial momentum. The higher the initial momentum of the packet (if positive), the easier the trans-

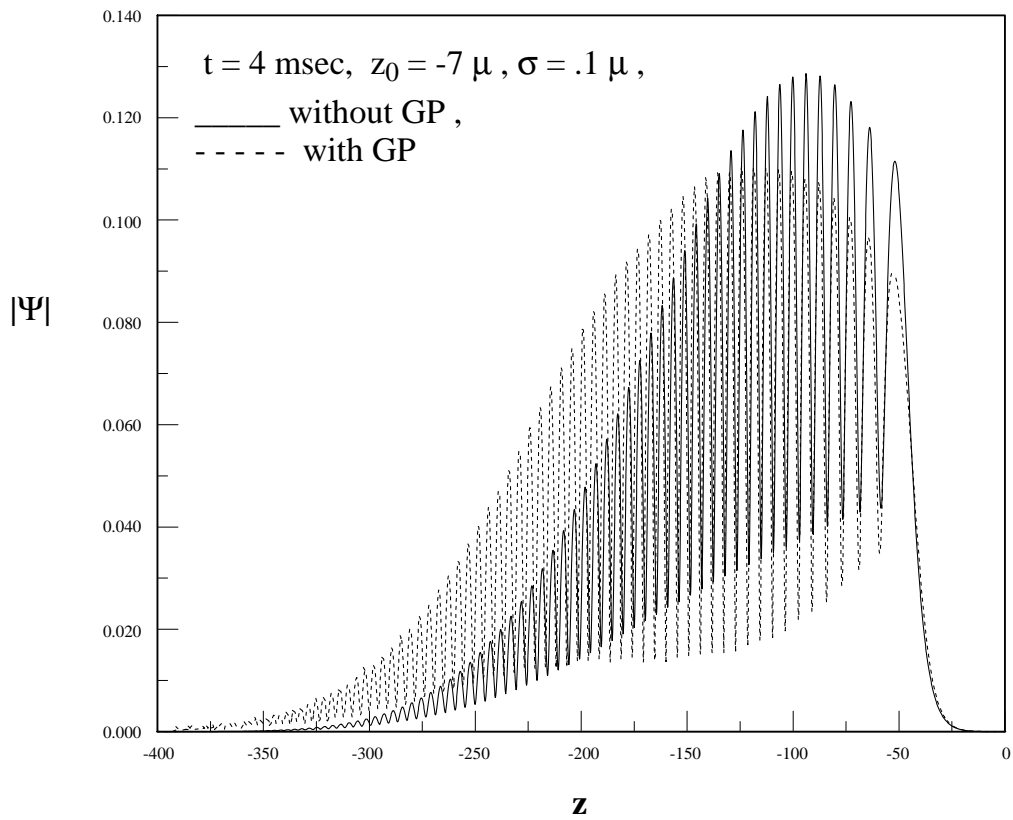


Figure 5: *Thin packets profiles after $t= 4 \text{ msec}$ of fall under a repulsive barrier with and without the Gross-Pitaevskii interaction.*

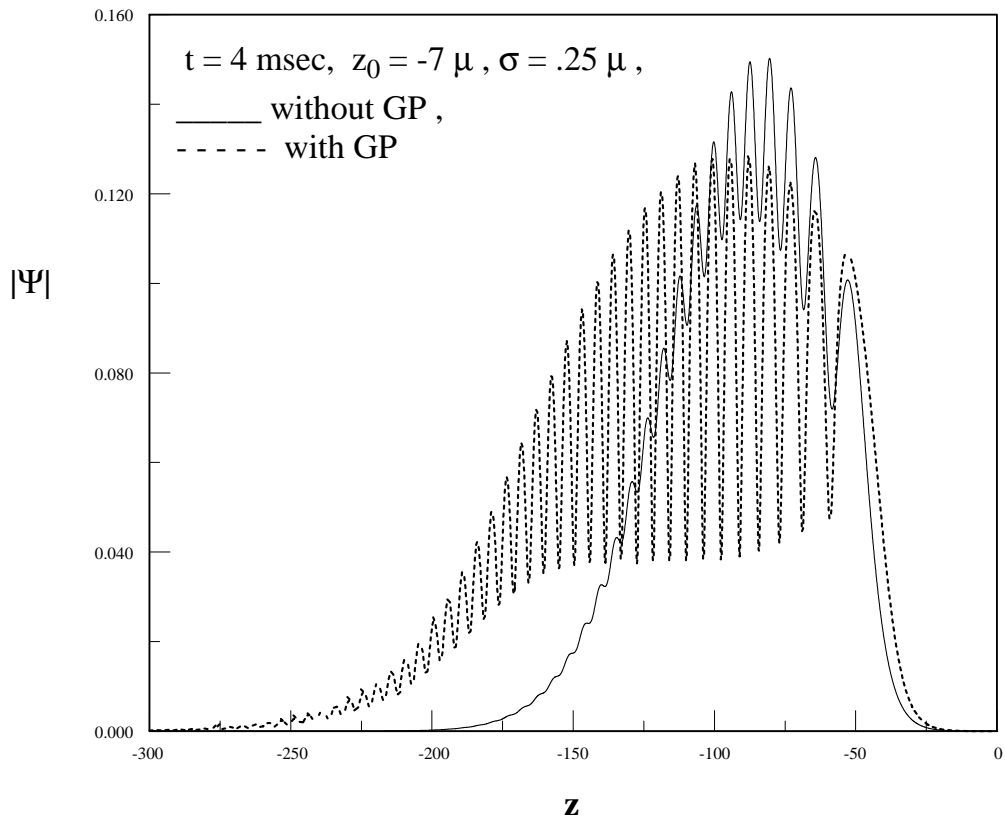


Figure 6: *Borderline packets profile after $t = 4 \text{ msec}$ of fall under a repulsive barrier without and including the Gross-Pitaevskii interaction.*

mission through the well. The differences arise then for packets thrown against the obstacle only at large momenta as compared to l_g^{-1} . This point will be dealt with in the future.

3 Theoretical approach to falling packets

The Airy function [21] is the solution of the Schrödinger equation for the propagation in a uniform field. Despite being named Airy packet, it is not normalizable and belongs to the set of wave functions in the continuum. It is the analog of a plane wave in free space.

The educational literature abounds in references to uses of this packet, both in the context of the *quantum bouncer*[17] and in the treatment of generalized Galilean transformations.[22]

For the solution of a packet falling on a mirror, the *quantum bouncer*, the Airy functions shifted to positions that have a zero at $z = 0$, serve as a basis to find the time development of an arbitrary initial packet. The non-normalizability of the Airy packet is of no hindrance here, because only the upper decaying part of the packet is used. Note however that an aspect that is ignored in the literature is the absence of orthogonality between the different shifted packets when integrated only over the positive z axis. This is perhaps not a severe problem, but was not taken into account in the works using the Airy packet for the *quantum bouncer* problem.[17]

The lower piece of the Airy packet is oscillatory and does not decay fast enough to serve as a basis for packets initially located under the mirror. Only when a continuum of energies (both positive and negative) is used, it is possible to expand an initial wavepacket located at $z < 0$ in terms of Airy functions.

Before analyzing the problem by means of Airy functions, we will develop a very simple approximation that allows the identification of the relevant length scale for the effect to occur.

We will resort to a set of solutions that connects directly to plane waves. This solutions are not stationary in the rigorous sense of the word, because they have a time dependent phase that is not linear in time. The solutions are derived by transforming a plane wave to an accelerating frame [22, 23, 24], namely

$$\begin{aligned} \chi_k(z, t) &= e^{i \phi} \\ \phi &= -m g z t + k \left(z + \frac{g t^2}{2} \right) - \frac{k^2}{2m} t - \frac{m g^2 t^3}{6} \end{aligned} \quad (5)$$

Direct substitution in the Schrödinger equation proves that this family of solutions solves the equation for a potential $V = m g z$.

Given that the initial wavepacket of eq.(2) may be expanded readily in plane waves that coincide with eq.(5) at $t=0$, the Schrödinger equation then insures that the subsequent propagation of the packet will be obtained by replacing the plane waves by the solutions in the gravitational potential of eq.(5).

We find the expression at all times for a freely falling normalized gaussian packet

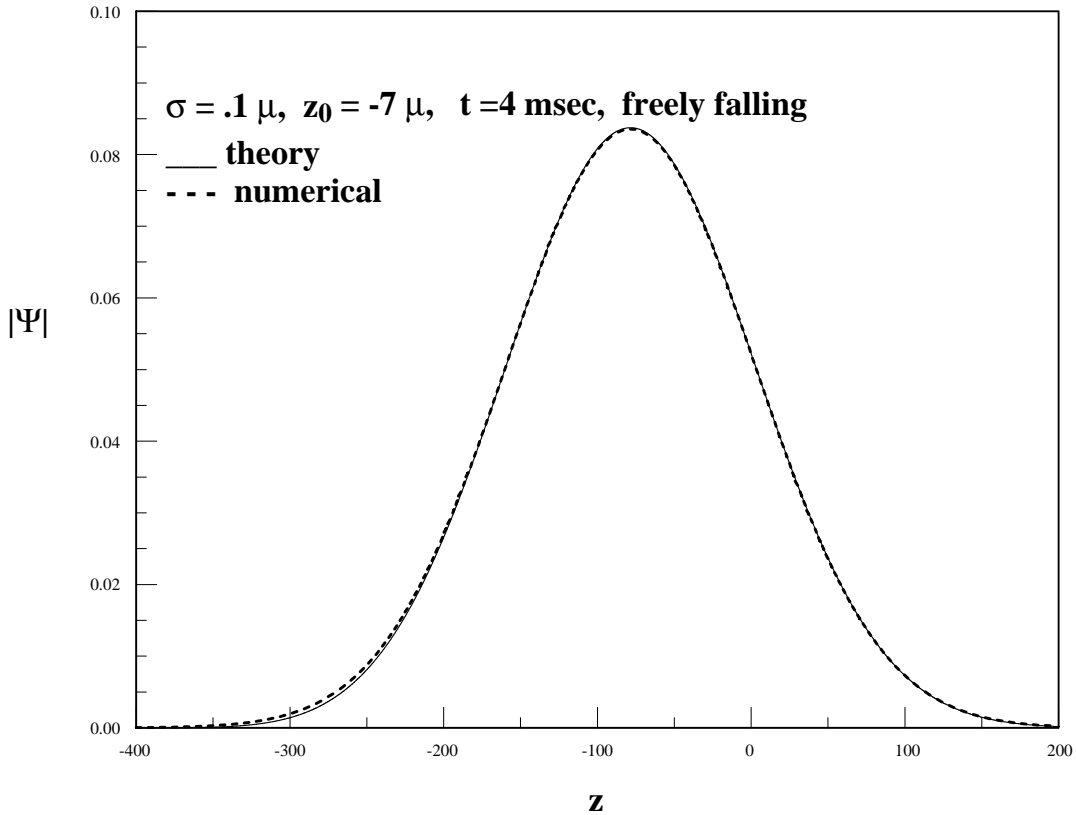


Figure 7: Profile of a packet of initial width $\sigma = 0.35 \mu$ and initial location $z_0 = -7 \mu$ in free fall after $t = 4 \text{ msec}$. Numerical calculation, dotted line, and theoretical formula of eq.(6) , full line

$$\begin{aligned}
 \Psi(z - z_0, t) &= \frac{e^{\xi} \chi_q(z - z_0, t) \sqrt{\sigma}}{\sqrt{\sqrt{2} \pi \sigma^2(t)}} \\
 \xi &= \frac{(z - z_0 + g t^2/2 - q/m t)^2}{4 \sigma^2(t)} \\
 \sigma^2(t) &= \frac{i t}{2 m} + \sigma^2
 \end{aligned} \tag{6}$$

Figure 7 depicts the comparison between the expression of eq.(6) and a numerical calculation. The agreement is satisfactory without any rescaling. It lends confidence in both the numerical scheme and the theoretical formulae.

At $t=0$ we can readily build a packet that solves the problem with the boundary condition of $\Phi(0) = 0$, corresponding to an impenetrable mirror at $z = 0$. Just an image packet located at $-z_0$ in the inaccessible region above the mirror will serve. The solution at $t=0$ then

becomes $\Phi(z, t = 0) = \Psi(z - z_0, 0) - \Psi(z + z_0, 0)$, with Ψ in eq.(6). Φ obeys the equation of motion and the boundary condition. It also coincides with the initial packet of eq.(2) in the allowed region of $z < 0$. Propagating Φ forward in time we obtain

$$\Phi(z, t) \approx \Psi(z - z_0, t) - \Psi(z + z_0, t) \quad (7)$$

We write the approximate sign, because the cancellation at $z = 0$ is only effective at short times. As soon as t increases, the wave function of eq.(7) does not vanish any more. Presumably, an infinite set of image packets is needed.

We could not find a closed analytical solution at all times. The solution of eq.(7) reproduces reasonably well the falling packets and distinguishes clearly between a packet narrower than l_g and one wider than l_g for z_0 of the order of a few packet widths. In order to see this we write the absolute value of eq.(7) for a packet with initial momentum $q = 0$ for $t \gg 2 m \sigma^2$

$$\begin{aligned} |\Psi(z, t)| &= A e^{\theta_1} \sqrt{\sin^2(\theta_2) + \sinh^2(\theta_3)} \\ \theta_1 &= -\frac{m^2 \sigma^2 \left((z + g t^2/2)^2 + z_0^2 \right)}{4 t^2} \\ \theta_2 &= \frac{m z_0 (z + g t^2/2)}{t} \\ \theta_3 &= \frac{m^2 \sigma^2 z_0 (z + g t^2/2)}{2 t^2} \end{aligned} \quad (8)$$

θ_3 is responsible for the blurring and loss of contrast of the diffraction pattern determined by the \sin function. The larger θ_3 the less visible are the oscillations. The criterion for the visibility of the pattern may then be written as $\max(\theta_3) \ll 1$. The maximum value of $-z$ is given by the descent of the packet and its spreading. Both are of the order of $\frac{g t^2}{2}$. We can then write the condition for the visibility of the interference fringes to be

$$\max(\theta_3) \approx \frac{m^2 \sigma^2 z_0 g}{2} \ll 1 \quad (9)$$

However, typically z_0 amounts to a few times the width of the packet, otherwise the oscillations will have a very large wavenumber, and will blur the pattern anyway.

Hence we can write eq.(9) as

$$\begin{aligned} \max(\theta_3) &\approx \frac{m^2 \sigma^3 g}{2} \ll 1 \\ &= \frac{\sigma^3}{4 l_g^3} \ll 1 \\ &\text{or} \\ \sigma &\ll l_g \end{aligned} \quad (10)$$

If we keep z_0 , eq.(10) becomes

$$\sigma \ll 2 \sqrt{\frac{l_g^3}{z_0}} \quad (11)$$

Eq.(11) demonstrates that the relevant borderline between a visible and blurred packet is $\sigma = \sqrt{\frac{l_g^3}{z_0}}$. A packet initially narrower than l_g located at a distance of a few times its width under a mirror will definitely display interference fringes. Eq.(8) also tells us that this pattern travels with the packet unscathed.

For long enough times we can improve upon the solution of eq.(7) in order to compensate for the inaccuracy in the cancellation at $z = 0$. The correction is achieved by multiplying the subtracted wave by a space independent, but time dependent admixture factor,

$$\begin{aligned} \Phi(z, t) &\approx \Psi(z - z_0, t) - \lambda \Psi(z + z_0, t) \\ \lambda &= \frac{\Psi(-z_0, t)}{\Psi(z_0, t)} \end{aligned} \quad (12)$$

By adding this factor we spoil the solution. Eq.(12) does not solve exactly the Schrödinger equation, whereas eq.(7) does. However, this inaccuracy decreases as a function of time, because $\lambda \rightarrow 1$ as $t \rightarrow \infty$. For times not so long it improves a little the agreement with the numerical results. It apparently compensates for the need of an infinite set of packets that insure the boundary condition at all times.

Figures 8 and 9 show the comparison between the formula of eq.(12) and the numerical results both for a thin packet and wider one.

The agreement is reasonable quite good for the wide packet and qualitatively reasonable for the thin packet. The formula captures the gross features, such as the absence of a diffractive structure for a wide packet and the wavenumber of the oscillations for a thin packet. It has one evident limitation: Lack of a sharp cutoff of the packet at small distances $-z$ for a thin packet. Nevertheless, the simple picture of single image packet is essentially correct.

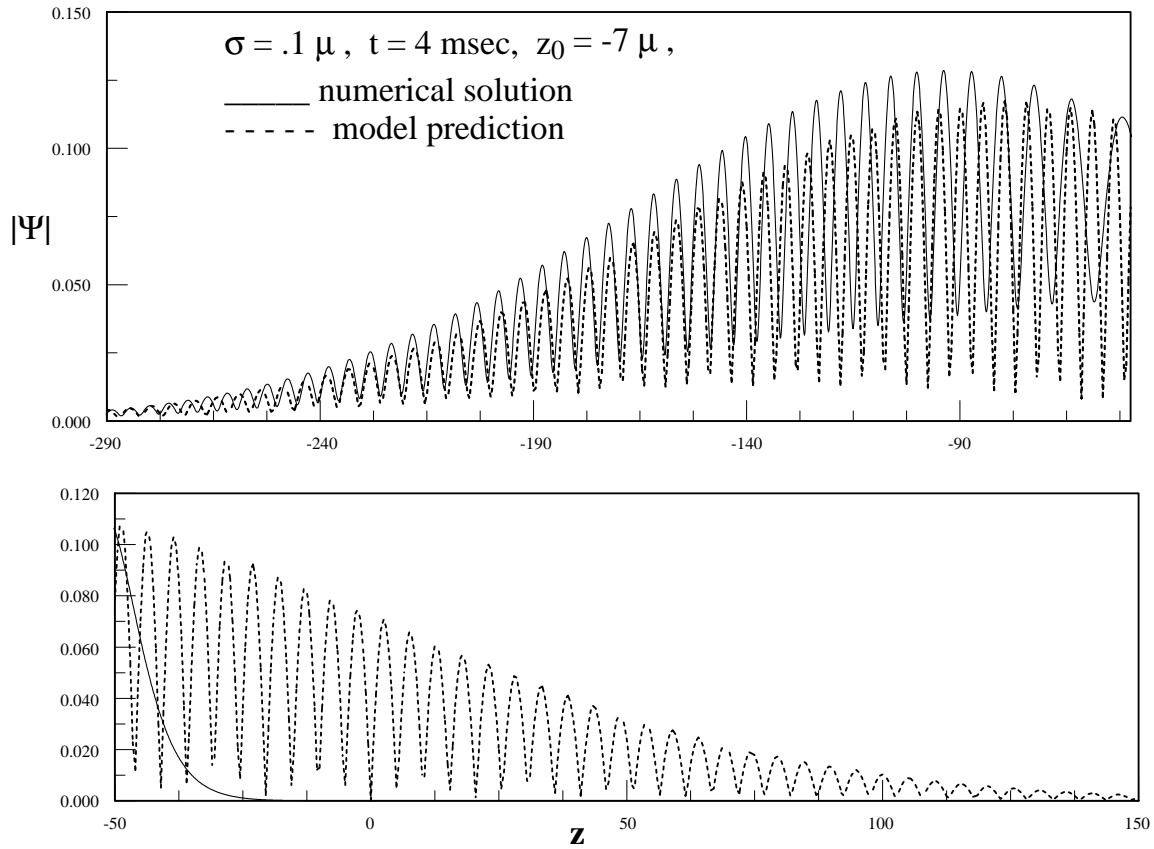


Figure 8: Thin packet profile of width $\sigma = 0.3 \mu$ after $t = 4 \text{ msec}$ falling under a reflecting mirror. Numerical calculation, solid line, and theoretical formula of eq.(12)

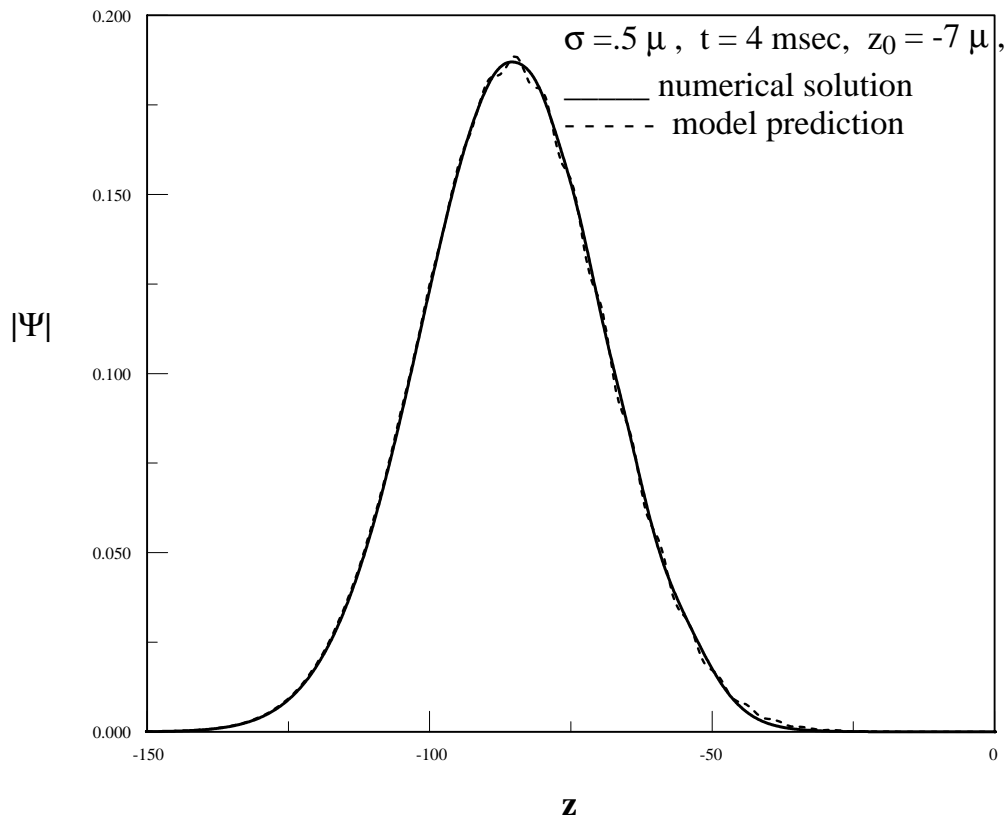


Figure 9: Wide packet profile of width $\sigma = 2 \mu$ after $t = 4 \text{ msec}$ falling under a reflecting mirror. Numerical calculation, solid line, and theoretical formula of eq.(12)

We now proceed to find a solution in terms of Airy functions.³

A solution of the mirror problem for $z < 0$ can be determined by means of a set of functions that solve the freely falling packet, namely linear combinations of the independent Airy functions *Ai* and *Bi*[26]. A set that implements the boundary condition of a vanishing wave function at the origin reads

$$\chi_a(x) = (Bi(a) Ai(x+a) - Ai(a) Bi(x+a))/\sqrt{Ai^2(a) + Bi^2(a)} \quad (13)$$

where $x = \frac{z}{l_g}$, $a = \frac{-E}{mgl_g}$, with E , the energy of a stationary solution $-\infty < a < \infty$. The functions obey

$$\int_{-\infty}^0 \chi_a(x) \chi_b(x) dx = \delta(a-b) \quad (14)$$

with δ , the Dirac δ function. The set is orthonormal and complete. The initial wave packet of eq.(2) is expanded in terms of the set above as

$$\begin{aligned} \Psi(z, t=0) &= \int_{-\infty}^{\infty} C(a) \chi_a(x) da \\ C(a) &= \int_{-\infty}^0 \chi_a(x) \Psi(x, t=0) dx \end{aligned} \quad (15)$$

The wave function at all times then becomes

$$\Psi(x, t) = \int_{-\infty}^{\infty} C(a) \chi_a(x) e^{i E t} da \quad (16)$$

For thin enough wave packets $C(a)$ may be obtained analytically by extending the integration to $+\infty$ and neglecting corrections of order $\gamma = \frac{\sigma}{l_g}$, with σ , the initial width of the packet. Under these approximations $C(a)$ becomes

$$C(a) = \left(2^3 \pi \gamma^2\right)^{\frac{1}{4}} l_g \exp((a+x_0) \gamma^2 + \frac{2 \gamma^6}{3}) \chi(a+x_0+\gamma^2) \quad (17)$$

where $x_0 = \frac{z_0}{l_g}$

Inserting this formula into eq.(16) we find the wave function at all times.

³The author wishes to express his gratitude for the extremely helpful remarks of one of the anonymous referees concerning the use of Airy functions

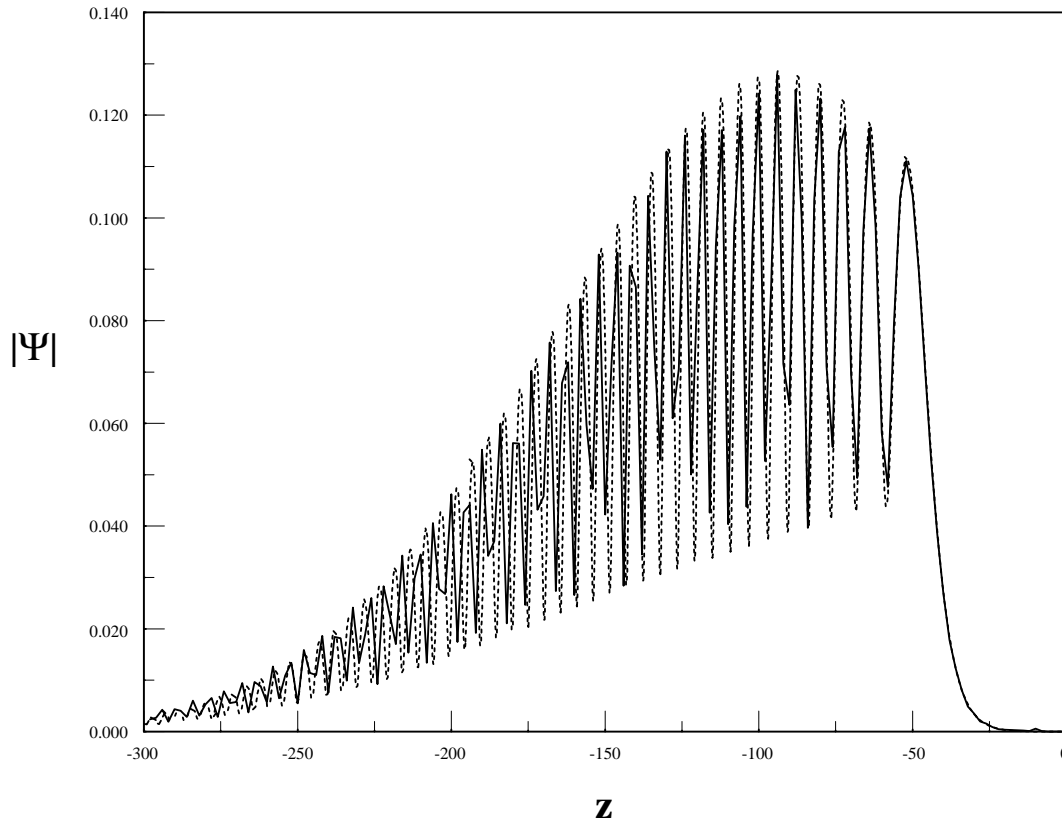


Figure 10: Numerical profile, dashed line, and, analytical solution of eq.(16), solid line for the thin packet of figure 1

Figures 10 and 11 present the comparison of the numerical calculation for a thin packet and a wider packet to the analytical formula of eq.(16) with the approximation of eq.(17). The thin packet fit is quite good, while for the wider packet there is a discrepancy in the height of the peak. This discrepancy is due to the fact that γ for a wider packet is not negligible and the formula of eq.(17) needs to be amended. However in both cases the basic feature of the existence and absence of a diffractive train is evident. It is worth mentioning that there is no rescaling of neither analytical nor numerical data points.

The long time behavior of the thin packet as compared to a wide packet remains unchanged for as far as we could integrate the time dependent Schrödinger equation numerically and still agrees with the analytical solution of eq.(16). We reached a time of 30 msec and the profiles just spread, but do not change in shape. At that time the center of the packet is around 4.5 mm below the mirror.

The integration of the equation becomes prohibitive beyond this time due to the strong oscillations in the wave function that require an increasingly smaller time step. The results

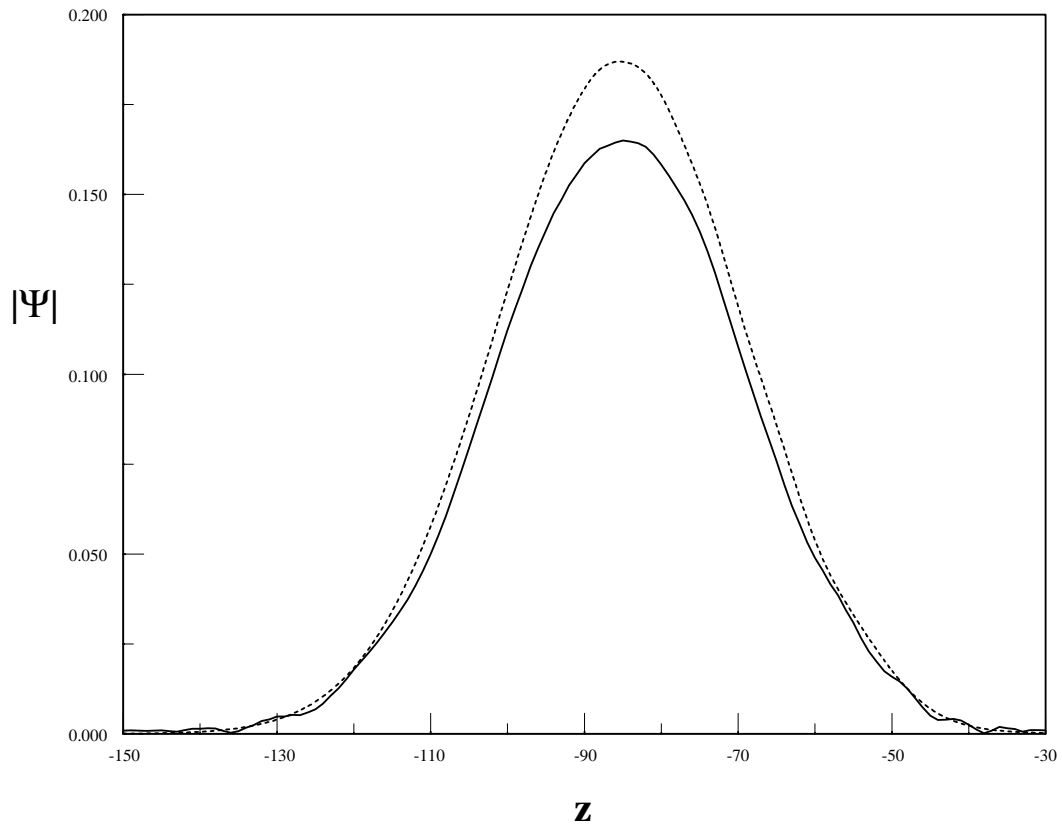


Figure 11: Numerical profile, dashed line, and, analytical solution of eq.(16), solid line for the wider packet of figure 1

however look quite firm. The diffractive structure persist to infinite times, as it was found for the wavepacket diffraction in space and time effect.[1]-[5]

In the next section we will provide some closing statements on the relevance of the falling packet effect for Bose-Einstein condensates and atom lasers.

4 *Summary*

We have found that a falling packet that is blocked by an obstacle *from above*, behaves differently depending on its initial spread. A packet wider than the gravitational mass dependent length scale l_g falls almost as a free packet except for a lag due to an effective attraction to the barrier or well, while a thin packet has a distinctive diffraction pattern that propagates with it analogous to the 'Wavepacket diffraction in space and time effect'[1]-[5].

We consider now a possible scenario to implement the findings of this work, and also take advantage of them for the purposes of creating an atom laser. Although there seems to be some controversy as to what an *atom laser* is[27], at a pedestrian level it would consist in a three stage machine: A feeding stage that pumps in atoms in an incoherent phase; a condensation cavity and a continuous output coupler. The investigation of these stages is as of today very advanced both theoretically and experimentally.[28]

We would like to point out that the results of this paper suggest an alternative avenue for the continuous output coupling of a Bose-Einstein condensate.

Basically, it consists of an orifice, a physical one or one drilled in the mesh of laser radiation that confines the condensate. Through the orifice the condensate can exit in a pencil-like thin jet of atoms. [12]

Position now a mirror above the atoms and let them fall freely while the feeding continues. It appears then that the outcome will be a coherent train of atoms having the characteristic oscillations found here, provided the width of the pencil is smaller than $\sqrt{l_g^3/z_0}$.

In order to see if this design works and check whether it fits the criteria of an atom laser set in ref.[27], we need to perform at least a two-dimensional calculation with a source term. This endeavor is currently underway.

5 *Acknowledgment*

I would like to thank the anonymous referees for very valuable remarks.

References

- [1] G. Kälbermann, Phys. Rev. **A60**, 2573 (1999).
- [2] G. Kälbermann, Jour. of Phys. **A 34**, 3841 (2001), quant-ph 9912042.
- [3] G. Kälbermann, Jour. of Phys. **A 34**, 6465 (2001), quant-ph 0008077.
- [4] G. Kälbermann, Wavepacket diffraction in the Kronig-Penney model, Jour. of Phys. **A 35**, 1045 (2002), cond-mat 0107522.
- [5] G. Kälbermann, Single and double slit scattering of wave packets, Jour. of Phys. **A**, to be published, quant-ph 0109111.
- [6] M. H. Anderson, J. R. Ensher, C. E. Wiemann, and E. A. Cornell, Science **269**, 198 (1995).
- [7] K. B. Davis, M. -O. Mewes, M. R. Andrews, N. J. Van-Druten, D. S. Durfee, D. M. Kurn and W. Ketterle, Phys. Rev. Lett. **75**, 3969 (1995)
- [8] M.-O. Mewes, M.R. Andrews, D. M. Kurn, D. S. Durfee, C.G. Townsend, and W. Ketterle, Phys. Rev. Lett.**78**, 582 (1997).
- [9] I. Bloch, T. W. Hänsch and T. Esslinger, Phys. Rev. Lett. **82**, 3008 (1999).
- [10] F. Gerbier, P. Bouyer, and A. Aspect, Phys. Rev. Lett. **86**, 4729 (2001).
- [11] V. Nesvizhevsky, H. Börner, A. Petukhov, H. Abele , S. Baessler, F. Ruess, T. Stöferle, A. Westphal, A. Gagarski, G. Petrov and A. Strelkov, Nature **415**, 297 (2002).
- [12] K. Bongs, S. Burger, G. Birkl, W. Ertmer, K. Rzazewki, A. Sanpera and M. Lewenstein, Phys. Rev. Lett. **83**, 3577 (1999).
- [13] A. Peters, K. Y. Chung and S. Chu, Nature **400**, 849 (1999).
- [14] M. Moshinsky, Phys. Rev. **88**, 625 (1952).
- [15] C. Brukner and A. Zeilinger, Phys. Rev. **A56**, 3804 (1997) , and references therein.
- [16] P. Szriftgiser, D. Guéry-Odelin, M. Arndt and J. Dalibard, Phys. Rev. Lett. **77**, 4 (1997).
- [17] J. Gea-Banacloche, Am. Jour. of Phys. **67**, 776 (1999), and references therein.
- [18] V. V. Dodonov , M. A. Andreatta, Phys. Lett. **A275**, 174 (2000).
- [19] F. Dalfovo, S. Giorgini, L. Pitaevskii and S. Stringari, Rev. of Mod. Phys. **71**, 463 (1999).

- [20] R.E. Grisenti, W. Schöllkopf, J. P. Toennies, C. C. Hegerfeldt, T. Köhler, Phys. Rev. Lett. **83**, 1755 (1999).
- [21] L. D. Landau and E. M. Lifschitz, *Quantum mechanics*, Pergamon, London, 1965, p. 79.
- [22] D. M. Greenberger, Am. Jour. of Phys. **48**, 256 (1980).
- [23] M. Wadati, Jour. Phys. Soc. Japan, **68**, 2543 (1999).
- [24] G. Vandegrift, Am. Jour. of Phys. **68**, 576 (2000).
- [25] O. Vallée, Am. Jour of Phys., **68**, 672 (2000).
- [26] M. Abramowitz and I. A. Stegun (eds.), *Handbook of Mathematical Functions*, Dover, NY (1972), section 10.4.
- [27] H. M. Wiseman, Phys. Rev. **A 56**, 2068 (1997); **57**, 674 (1998).
- [28] R. J. Ballagh, C.M. Savage, Mod. Phys. Lett. **B14**, supplement **S**, 153 (2000), arXiv cond-mat/0008070.